Structural Design of Nonuniform Metasurface to Mimic the Deformation Behavior of Human Skin at Highly-Stretched Joint Area

†*Yafeng Han[1], Changmeng Liu[1], Shuyuan Ma[1], Jiping Lu[1], Ying Liu[1], and Wenfeng Lu[2]

[1]School of Mechanical Engineering, Beijing Institute of Technology, Beijing 100081, China

[2]Department of Mechanical Engineering, National University of Singapore, 9 Engineering Drive 1, 117975, Singapore

†Corresponding author & *Presenting author: hanyafeng@bit.edu.cn

Abstract

Developing new generation nonuniform metasurface with skin-like stretchability and conformability has become the research hotspot in many areas, such as bio-sensoring, medical bandages, wearable devices and soft robotics. In this study, a computational method was proposed to design nonuniform 2D metasurface, which could perform a similar deformation as the target skin surface during the rotation of joint. Considering the nonuniform auxetic deformation behavior of the skin around joint area, the designed metasurface should also have the same Poisson's ratio (PR) distribution. By mapping unit cells with different PR to the target surface, the obtained structure would have the same mechanical property and deformation behavior as the covered skin. With the unique capabilities of additive manufacturing (AM), the generated 2D metasurface can be easily fabricated. Especially, new generation wearable electronics with superior conformability was developed based on this nonuniform structure. Besides, the proposed method is also promising to be applied to design novel biomaterials, such as wearable electronics, smart bandage, skin scaffold, *etc.*

Keywords: Nonuniform metasurface, Poisson's ratio distribution, nonuniform auxetic deformation, additive manufacturing

1. Introduction

Thin film structures are used in diverse technological applications such as stretchable electronics, soft robotics, smart bandages, wearable devices and living devices. In all these areas, achieving a "human-skin-like" deformation behaviour is the main design objective of the manufactured film structure. Mainly, researches have tried to solve this problem from two aspects: soft materials or stretchable structures.

To obtain better comfortability, many researchers in stretchable electronics area have dedicated to develop new materials with better stretchability. As early as 1994, Garnier, Hajlaoui, Yassar and Srivastava [1] had fabricated a field-effect transistor from organic materials with printing technology. This flexible device can be bended or twisted without causing much difference on the conductivity. From then on, organic electronics have proven useful in a number of applications, such as light patterning techniques and organic semiconductors [2]. The strain sustainability of organic electronics, despite much better than common wafer-based devices, is still not enough to conform the complex 3D surface of human body [3].

Changing the structure of the film metasurface is another way to achieve better stretchability. The most commonly applied strategy is converting the traditional all solid surface into "wavy"

structures [4]. In the research [5] of Kim et al., several different circuit designs were introduced to construct the “epidermal electronic system”. While, all these circuit patterns were developed based on the significant stretchability of “wavy” structure. Someya et al. [6] manufactured a networks of pressure and thermal sensors with conductive rubber. Similarly, the impressive skin-like conformability and flexibility was gained from the “wavy” layout of the material. Besides, many fabric-based electronics [7,8] also have shown good conductivity during deformation. The reason is that the conductive wires enabled in fabrics are always at a loose- knit state, which is still a nonconstant “wavy” structure essentially. To eliminate this deformation property difference between substrate and conductive wires, Jeong, Kim, Cho and Hong [4] introduced the “wavy” structure to the construction of both substrate and electrode. This wavy substrate was fabricated through casting, and base material was chosen as PDMS for better flexibility. Consequently, the deformation behaviour of both substrate and silver electrodes can be maintained as uniform, which will dramatically decrease the sheer stress at the connection areas. Similarly, a spiral shape wiring system was proposed in the study of Sawada et cl. [9], and both substrate and conductive wires were manufactured into same structure. The only difference is that the spiral shaped substrate was made of photosensitive polyimide and exposed with copper foil. Resistance of the constructed stretchable wiring network changed little, even after 200 cycles of 20% stretching.

Compared with stretchability, conformability is a more important property for wearable devices or medical bandages. Especially, some joint areas of human body have very complex 3D surfaces, and skin around these areas always bear extremely high stretching. Besides, the skin at joint area is always unevenly stretched at all directions, which means this is a nonuniform auxetic deformation. To mimic such a unique deformation behaviour, negative Poisson’s ratio (NPR) structures became necessary to construct the suitable wearable electronics [10]. Yang, Choi and Kamien [11] utilized fractal cuts to develop super conformable materials that could be applied to design stretchable electronics. After the proposed fractal cut process, a common silicone rubber sheet can be easily stretched and conformed to a spherical surface. In Vogiatzis, Ma, Chen and Gu’s study [12], topology optimization method was applied to design NPR structures with optimized conformability. The optimized 2D metasurface can conform to the complex surface of a human face, which provided great potential for the structural design of wearable electronics. However, all these conformable NPR structures were uniformly constructed. Considering the nonuniform auxetic deformation of the skin, there will beinevitable deformation behaviour difference between the thin film and human skin. This difference will definitely cause sheer stress at the connection area between substrate and skin surface, which will reduce the stability of the device and may even cause detachment of the wearable electronic. To make sure the designed metasurface have the same deformation behaviour as the target skin surface, substrate structures with nonuniform PR distribution [13– 15] can be introduced.

In this study, a novel method was proposed to design and manufacture thin film structures with customized deformation behaviour, which can conform with the highly-stretched skin surface at human joint areas. By analysing the deformation behaviour of the skin during the rotation of joint, elongation (along the rotation surface) and expandation (vertical to the rotation surface) values of each small subsurface were measured. With this deformation data of all subsurfaces, strain and PR distribution of the target skin were calculated. To mimic the nonuniform PR distribution of the skin, the structure of substrate was organized by connecting unit cells with different PR values. Tuneable PR of unit cell was obtained by changing the interior angle of re- entrant honeycomb structure, which was still a mutation of “wavy” structures. Skin around a person-specific elbow was chosen as the target surface. After deformation analysis and structural construction, finite element analysis (FEA) was

conducted to validate the conformability of the designed nonuniform substrate. With PolyJet printed flexible nonuniform metasurface, stretching test was carried out to measure deformation behaviour, and both computational and experimental tests have shown a perfect conformability.

2. Materials and methods

2.1 Materials

To enhance the stretchability and flexibility of the elastomer film, rubber-like material Agilus30 was selected. This newly developed material is one of the most flexible materials available for Objet Connex 260 (Stratasys Inc., Edina, MN, USA). As tested in [16], this material can be assumed as linear elastic when the applied strain is smaller than 100%, and the material Young's modulus is 423MPa and Poisson's ratio is 0.34.

2.2 General processes of the proposed method

In this study, a structural design method was proposed to develop metasurface structure with nonuniform PR distribution to conform with skin surfaces around highly stretched joint areas. Particularly, the method was mainly composed of six steps as shown in Figure 1. Firstly, 3D scanning was conducted to get the point cloud data of the skin surface around joint. The joint surface was scanned at two positions: fully-straightened and fully-bended. The fully-straightened position was set as initial state with assumed strain and deformation of zero. On the other hand, the fully-bended position was the objective state. From the initial state to the objective state, the deformation behaviour of the skin can be analysed. The skin surface was descriptive into finite subsurfaces to analyse how the strain and deformation was distributed over the surface area. By setting as joint bending direction the applied strain direction, PR of each subsurface could be calculated easily. To mimic the nonuniform auxetic deformation of the skin, the PR distribution in the substrate should also be nonuniform correspondingly. As been done in our previous research [17], re-entrant honeycomb structure was introduced to achieve tuneable PR by manipulating the interior angle of each unit cell. The size of unit cell was defined based the geometry of subsurface to make sure that each subsurface was covered by one unit cell. Considering the relative large deformation, geometrically nonlinear FEA was applied to get the relationship between unit cell's PR and the interior angle. With this relationship, Unit cells with the same PR values were mapped to cover the all the subsurfaces of the skin. Both computational and experimental tests were conducted to validate the conformability of the design substrate structure. Two comparison structures, uniform NPR anduniform PPR, were also tested to demonstrate whether the generated nonuniform structure had better conformability.

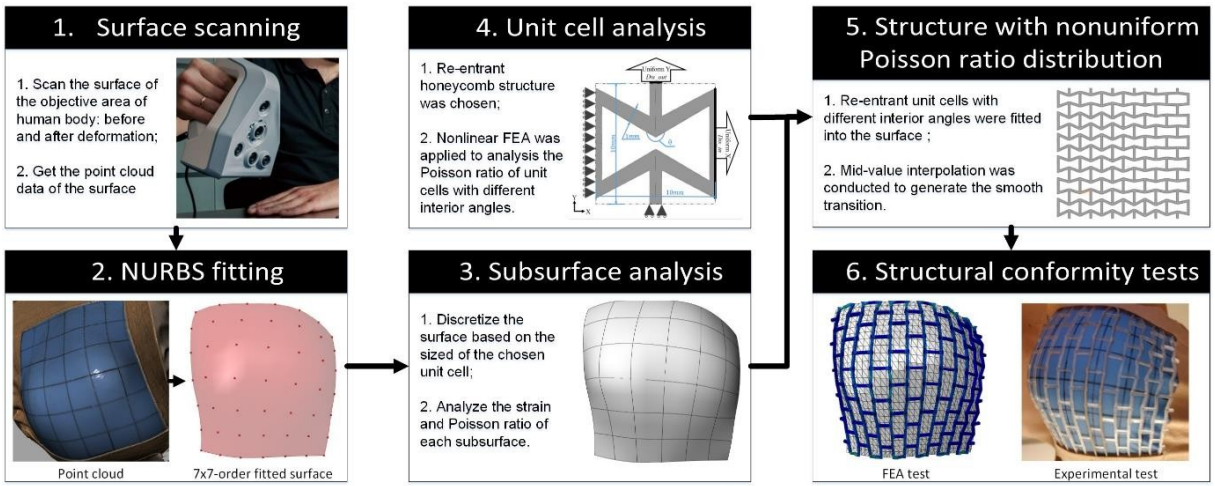

Figure 1. General process of the proposed design and manufacturing method

2.3 Skin surface scanning and analysis

Commonly, human skin is in the form of complex 3D surface. It is extremely challenging to model the such a complex geometry manually, especially with the consideration of the slight difference between each individual. To customize the metasurface structure for each person-specific design, 3D scanning was utilized in this study to collect the geomaterial data of the target skin surface. An ArtecTM Space Spider (Artec Inc., Luxembourg) was applied to conduct the 3D scanning of the skin surface. This portable/handheld scanner has outstanding capabilities to render complex geometry, sharp edges and thin ribs.

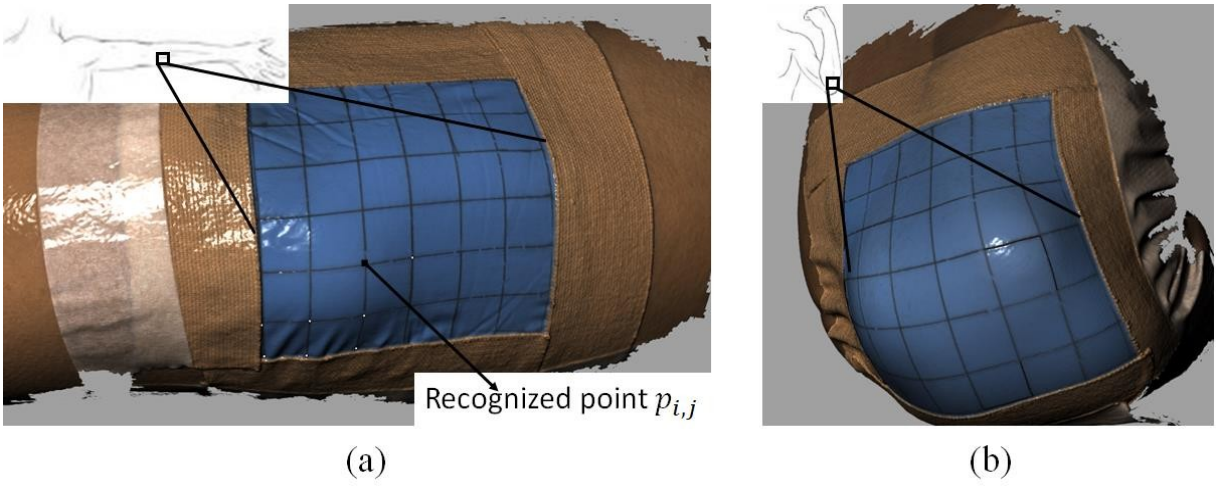

Figure 2. Scanning results of the skin surface around a person-specific joint area:

(a) straightened state, (b) bended state.

Figure 2 shows the scanning results of the skin surface around a person-specific joint area. For the convenience of feature recognition, a blue rubber film with marked uniform grid was attached to the target area. Considering the difficulty of analysing the point cloud data, curvilinear surface fitting was necessary. Nonuniform Rational B-splines (NURBS) are mathematical models usually used in computer graphics [18], which was chosen to mathematically represent the scanned surface. However, it's not possible to fit NURBS surface to the whole point cloud directly because of the massive separated point data and requirement of NURBS surface approximation. To make the surface approximation more efficiently computer aided feature recognition was introduced to find the coordinates of all intersection points "+" in the scanning results, as shown in Figure 2a. By fitting a NURBS

surface that crossed all the recognized points, geometrically analysis could be processed. Detailedly, for a 3D NURBS with the order of (p, q), the mathematical definition is given in Equation (1).

$$S(u,v) = \frac{\sum_{x=0}^{n}\sum_{y=0}^{m} N_{x,p}(u)N_{y,q}(v)w_{x,y}C_{x,y}}{\sum_{x=0}^{n}\sum_{y=0}^{m} N_{x,p}(u)N_{y,q}(v)\,w_{x,y}}$$
$$0 < u, v < 1 \quad (1)$$
$$p \leq n; q \leq m$$

where, n and m denote the number of control points at direction of u and v. To construct a NURBS surface with the order of (p, q), the number of control points must be larger or equals to the order. $N_{x,p}$ are the non-rational B-spline basis functions defined on the knot vectors. $C_{x,y}$ is the coordinate of control point, and $w_{x,y}$ is the weight of the point. In this paper, to obtain a linear solution, all the weights were set to 1. With the coordinates of all recognized points $P_{i,j}$, the NURBS surface can be approximated in the least-squares sense:

$$\min \sum_{i=1}^{k}\sum_{j=1}^{l}(P_{i,j} - S(u_i, v_j)) \quad (2)$$

where, k and l are the number of recognized points on the surface at the direction of u and v respectively. With a total number of fitting points equals $k \times$, a 3D NURBS was approximately constructed. Figure 3a shows a 7 × 7 order NURBS that fitted from 7 × 7 points on the scanned skin surface of the bended elbow (Figure 2b). The fitted NURBS had a significant advantage that it can be evenly subdivided into any number of subsurfaces, with mathematical interpolating process. As demonstrated in Figure 3b & 3c, the fitted NURBS was divided into smaller subsurfaces and each subsurface still could represent the deformed geometry of a smaller skin area.

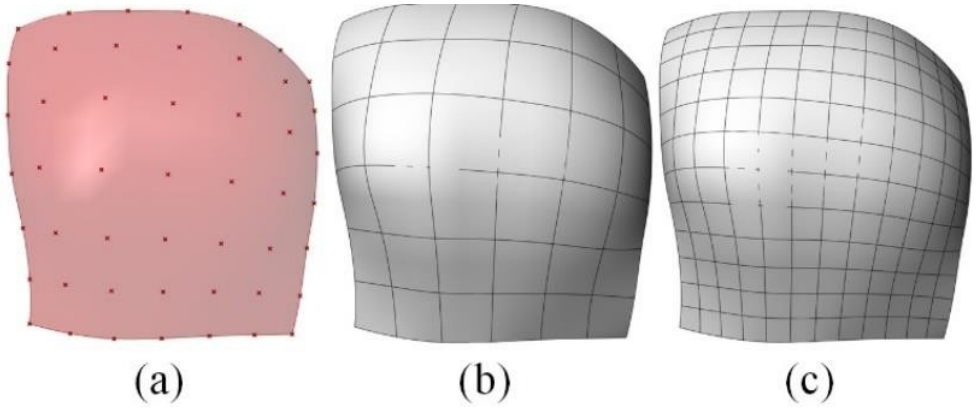

Figure 3. NUMBS fitting and dividing. (a) a NUMBS fitted from 7 × 7 points on the surface. (b) the fitted NUMBS was divided into 6 × 6 subsurfaces. (c) the fitted NUMBS was divided into 12 × 12 subsurfaces.

To analysis the deformation behaviour of the target skin area, the straightened joint was set as the initial state (Figure 2a). As this state, the skin was assumed as non-stretched and the side-lengths of all square subsurfaces were kept as uniform with the value of l_{int}, as shown in Figure 4a. The side-lengths of each square would keep changing along with the bending of the joint. When the maximum bending was applied as suggested in Figure 2b, the skin would also be stretched to the maximum extent. The side-lengths of each subsurface of the deformed skin were measured based on the interpolation of the NURBS. As marked in Figure 4b, the length

of each edge of subsurface $SubS_{w,z}$ became different to each other.

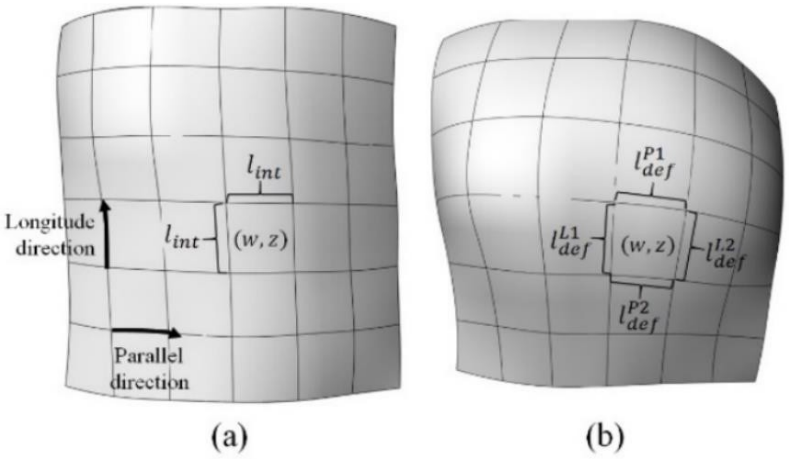

Figure 4. Measuring the side-length of each subsurface: (a) initial state, (b) target state.

The length change of each edge represented the elongation (along longitude direction) and expandation (along parallel direction) of the subsurface. To simplify the deformation analysis, the deformation of the subsurface was assumed as axisymmetric. Therefore, average elongation values were used to calculate the applied strain of each subsurface, as demonstrated in Equation (3). Besides, Poisson's ratio of the subsurface could also be derived from the side-lengths of the deformed subsurface (Figure 4b) with Equation (4).

$$\varepsilon_{w,z} = (l_{def}^{L1} + l_{def}^{L2} - 2l_{int}) \Big/ 2l_{int} \tag{3}$$

$$\nu_{w,z} = (l_{def}^{P1} + l_{def}^{P2} - 2l_{int}) \Big/ (l_{def}^{L1} + l_{def}^{L2} - 2l_{int}) \tag{4}$$

As shown in Figure 5, (w,z) is the number of the analysed subsurface. l_{int} denotes the initial length of all subsurface edges. Respectively, l_{def}^{L} and l_{def}^{P} represent the elongation and expandation the subsurface after the bending of joint. Even though the calculation of both strain and PR was based on the assumption of axisymmetric deformation, the influence could be ignored if the size of subsurface was small enough. By analysing all the subsurfaces one by one, the nonuniform strain and PR distribution of the target skin surface was demonstrated.

2.4 Unit cell analysis and structure generation

To mimic the nonuniform deformation behaviour of the skin around joint area, the designed metasurface should also possess a similar PR distribution to generate no sheer stress over the connection area of substrate and human skin. As the basic strategy of the proposed method, the nonuniform of PR distribution was achieved by connecting unit cells with different PR into an integrated structure. The PR of re-entrant honeycomb structure can be easily modified from negative to positive by just changing the interior angle [17]. To analyse the PR of unit cells with different interior angle θ and under different strain, geometrical nonlinear FEA was conducted. Agilus30 was selected as the base material, and the load and boundary conditions of the analysis is demonstrated in Figure 5. The unit cell can cover a square area with side-length of $lcell$ = $10mm$. By applying a $+X$ direction displacement Dis_in on the left boundary of the unit cell, the output displacement Dis_out was measured. The applied strain $\varepsilon cell$ and PR $\nu cell$ of the unit cell was calculated with Equation (5) & (6).

$$\varepsilon_{cell} = Dis\_in / l_{cell} \tag{5}$$

$$\nu_{ce\square\square l} = Dis\_out/is\_out \quad (6)$$

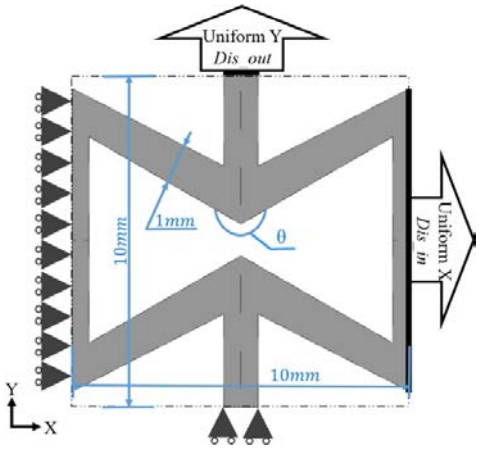

Figure 5. Load and boundary conditions for the nonlinear FEA of unit cell

Thirteen unit cells with different interior angle, form $\theta = 120°$ to $\theta = 240°$, were analysed. Because geometrical nonlinearity was considered, PR of each unit cell was different with the change of applied strain, as shown in Figure 7. With the summarized "ν-θ-ε" relationship in Figure 7, the nonuniform substrate structure was generated by assigning the corresponding unit cell to mimic the properties of each subsurface, letting $\varepsilon_{cell} = \varepsilon_{w,z}$ and $\nu_{cell} = \nu_{w,z}$.

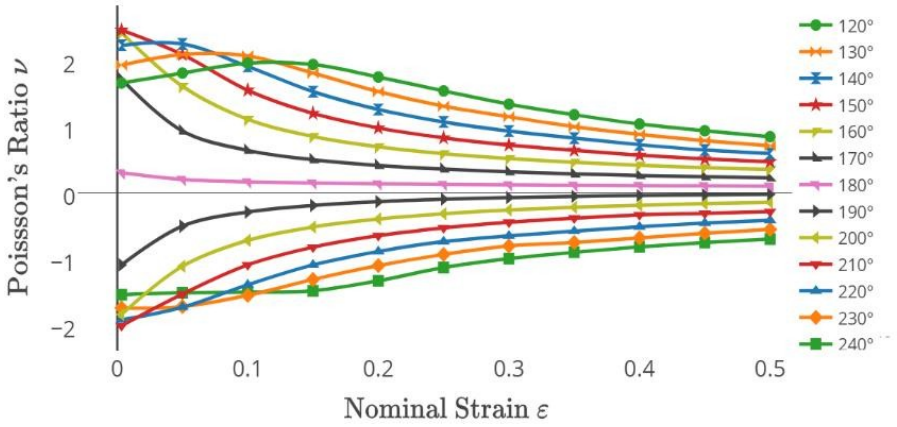

Figure 6. The relationship between applied strain, PR value and unit cell's interior angel

3. Numerical and experimental validation

To validate the proposed structural design method, a more challenging task, designing a nonuniform metasurface structure that suitable for a person-specific elbow, was introduced. The skin surface of the person-specific elbow is shown in Figure 2. A $60 \times 60mm^2$ area was chosen as the target surface to the attach the film structure. With the surface scanning and analysis method discussed in Section 2.3, the point cloud data of the scanned target surface was fitted into a 7 × 7 order NUMBS (Figure 3a). The reason why such a relatively low order was chosen to represent this NUMBS is that the precision of our equipment can only guarantee the stretchability and conductivity of the structure with relatively large unit cell (Figure 5).

For each subsurface of the target NUMBS, length of each edge was measured. Based on Equation (3) & (4), applied strain and PR of the subsurface can be obtained. Figure 7b shows the length of each edge for subsurface $SubS_{1,1}$. With Equation (3) and (4), we could get the

applied strain ($\varepsilon_{1,1} = 0.175$) and PR ($\nu_{1,1} = -0.543$) of the subsurface $SubS_{1,1}$. From the resulted "ν-θ-ε" relationship summarized in Figure 6, the corresponding unit cell (with $\varepsilon_{cell} = 0.175$ & $\nu_{cell} = -0.543$) has the interior angle of $\theta_{cell} = 206.8°$, as shown in Figure 7c. As a result, this unit cell will be mapped to the position of $SubS_{1,1}$. One by one form $SubS_{1,1}$ to $Sub\square\square_{6,6}$, every subsurface were analysed and unit cell with the same deformation behaviour was mapped. The stretched strain and PR of all subsurfaces were summarized in Appendix 1. Besides, the corresponding interior angle of unit cell were also listed in the appendix. By connecting all the unit cells, the nonuniform structure of substrate were generated.

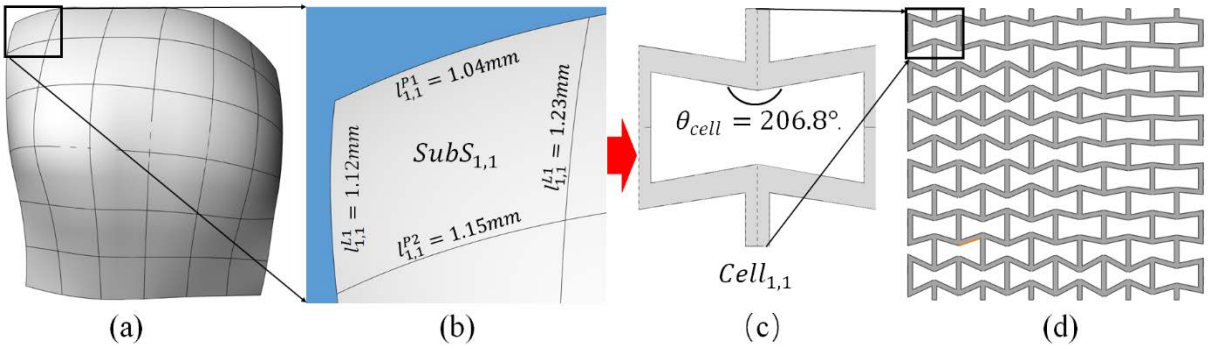

Figure 7. The construction process of the nonuniform substrate. (a) shows the geometry of target NUMBS. (b) & (c) demonstrates the detailed generation process of the unit cell $Cell_{1,1}$. (d) is the layout of the final substrate structure.

First, nonlinear FEA was conducted to test the conformability of the generated substrate. The setup of the test is illustrated in Figure 8a. The fitted NUMBS was defined as rigid body, and user-defined displacements were applied on both ends of the flexible substrate. All these displacements were defined through user-subroutines in Abaqus, and the objective was to make sure two ends of substrate were exactly connected with top and bottom edges of the target NUMBS. The dynamic-explicit solver was utilized to solve this nonlinear problem. As comparisons, structures with both uniform PPR and uniform NPR were also analysed. All these three FEA results were showed in Figure 8. To quantitatively evaluate the conformality of each stretched substrate, reciprocal of the maximum distance between the substrate and the edge of objective surface was introduced. As listed in Table 1, the substrate with nonuniform PR distribution had the best conformality to cover the target skin surface.

Table 1. FEA resulted maximum distance and conformability of all three structures.

Substrate structure	Uniform PPR	Uniform NPR	Nonuniform
Maximum distance (mm)	9.51	3.12	0.92
Conformability (mm^{-1})	0.039	0.321	1.097

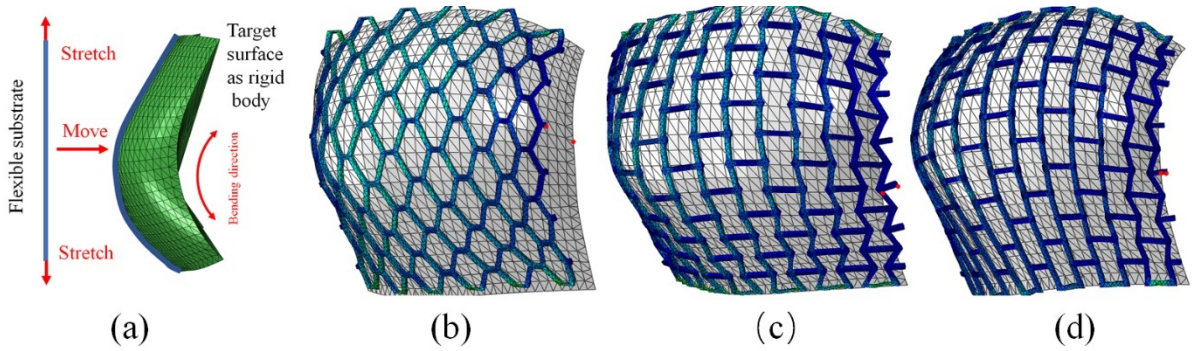

Figure 8. (a) illustrates the initial state and boundary conditions of the dynamic FEA test. Respectively, (b), (c) and (d) show the FEA results of uniform PPR, uniform NPR and nonuniform substrates.

Experimental tests were also carried out to validate both the conformability and conductivity of the designed nonuniform structure. Still, uniform NPR and PPR structure were tested as comparison. The deformation results of all three substrates were demonstrated in Figure 9, and measured maximum distance and resulted conformability were listed in Table 2. Same as the FEA test, the deformation behaviour of the designed nonuniform substrate wes more alike to the target skin. With large gap areas or out-of-bound areas (rad circle areas in Figure 9), it needs extra forces be applied on both free boundaries for uniform structures to obtain better conformation. However, this will bring sheer stress at the substrate-skin connection area, which will decrease the stability of the wearable devices dramatically. Therefore, the nonuniform structure, with a similar deformation behaviour to the target skin, is the most preferred design for wearable electronics at highly-stretched joint areas. Moreover, this nonuniform structure can exactly conform with the target surface without causing any wrinkle on the skin, which is impossible for those uniform structures, such as bulking structures, open-mesh structures, sponge structures *etc.*

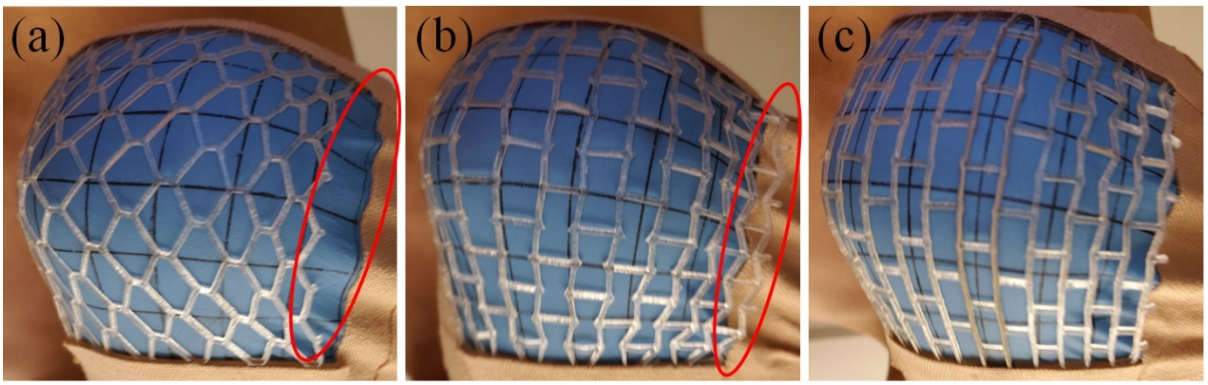

Figure 9. Experimental tests of the conformability of three different structures: (a) uniform PPR, (b) uniform NPR, and (c) nonuniform.

Table 2. Experimentally resulted maximum distance and conformability of all three structures.

Substrate structure	Uniform PPR	Uniform NPR	Nonuniform
Maximum distance (mm)	7.02	5.60	1.32
Conformability (mm^{-1})	0.142	0.179	0.758

4. Conclusions

In this paper, a novel method was proposed to develop metasurface structure for highly-

stretched skin around joint areas. Both structural design and manufacture processes were included in this novel method. The PR distribution in the designed thin film structure was organized base on the analysis of the target skin surface. By mapping re-entrant unit cells with different PR to the subsurface areas with the same mechanical properties, the generated structure could mimic the deformation behaviour of the target skin. As a result, the sheer stress at the connection areas between substrate and the attached skin would be eliminated, which is the main challenge for those common film structures with uniformly distributed material. This property brings good flexibility and conformability to the designed metasurface. The proposed structural design method can be introduced to solve problems in different areas. One of our future works is to develop patient-specific skin scaffold that can perfectly conformed to the 3D complex surface of human body. Soft robotics and 4D printing are also the possible application areas.

References

[1] F. Garnier, R. Hajlaoui, A. Yassar, P. Srivastava, All-Polymer Field-Effect Transistor Realized by Printing Techniques , Sci. . 265 (1994) 1684–1686. doi:10.1126/science.265.5179.1684.

[2] E. Menard, M.A. Meitl, Y. Sun, J.U. Park, D.J.L. Shir, Y.S. Nam, S. Jeon, J.A. Rogers, Micro- and nanopatterning techniques for organic electronic and optoelectronic systems, Chem. Rev. 107 (2007) 1117–1160. doi:10.1021/cr050139y.

[3] J.H. Ahn, J.H. Je, Stretchable electronics: Materials, architectures and integrations, J. Phys. D. Appl. Phys. 45 (2012). doi:10.1088/0022-3727/45/10/103001.

[4] J. Jeong, S. Kim, J. Cho, Y. Hong, Stable stretchable silver electrode directly deposited on wavy elastomeric substrate, IEEE Electron Device Lett. 30 (2009) 1284–1286. doi:10.1109/LED.2009.2033723.

[5] D.-H. Kim, N. Lu, R. Ma, Y.-S. Kim, R.-H. Kim, S. Wang, J. Wu, S.M. Won, H. Tao, Islam, K.J. Yu, T. Kim, R. Chowdhury, M. Ying, L. Xu, M. Li, H.-J. Chung, H. Keum, M. McCormick, P. Liu, Y.-W. Zhang, F.G. Omenetto, Y. Huang, T. Coleman,

[6] J.A. Rogers, Epidermal Electronics , Sci. . 333 (2011) 838–843. doi:10.1126/science.1206157. T. Someya, Y. Kato, T. Sekitani, S. Iba, Y. Noguchi, Y. Murase, H. Kawaguchi, T. Sakurai, Conformable, flexible, large-area networks of pressure and thermal sensors with organic transistor active matrixes, Proc. Natl. Acad. Sci. 102 (2005) 12321– 12325. doi:10.1073/pnas.0502392102.

[7] Q. Wu, J. Hu, A novel design of wearable thermoelectric generator based on 3D fabric structure, Smart Mater. Struct.,. at press (2017). https://doi.org/10.1088/1361- 665X/aa5694.

[8] W. Zeng, L. Shu, Q. Li, S. Chen, F. Wang, X.M. Tao, Fiber-based wearable electronics: A review of materials, fabrication, devices, and applications, Adv. Mater. 26 (2014) 5310–5336. doi:10.1002/adma.201400633.

[9] S. Sawada, Y. Tomita, K. Hirano, H. Morita, T. Ichiryu, M. Nomura, K. Kawakita, Novel wiring structure for 3D-conformable devices, 2016 Int. Conf. Electron. Packag. ICEP 2016. (2016) 124–128. doi:10.1109/ICEP.2016.7486795.

[10] X. Ren, R. Das, P. Tran, T.D. Ngo, Y.M. Xie, Auxetic metamaterials and structures: a review Auxetic metamaterials and structures: a review, Smart Mater. Struct. (2018). http://iopscience.iop.org/article/10.1088/1361-665X/aaa61c/pdf.

[11] S. Yang, I.S. Choi, R.D. Kamien, Design of super-conformable, foldable materials via fractal cuts and lattice kirigami, MRS Bull. 41 (2016) 130–137. doi:10.1557/mrs.2016.5.

[12] P. Vogiatzis, M. Ma, S. Chen, X.D. Gu, Computational design and additive manufacturing of periodic conformal metasurfaces by synthesizing topology optimization with conformal mapping, Comput. Methods Appl. Mech. Eng. 328 (2018) 477–497. doi:10.1016/j.cma.2017.09.012.

[13] Y. Han, W.F. Lu, Structural design of wearable electronics suitable for highly-stretched joint areas, Smart Mater. Struct. 27 (2018). doi:10.1088/1361-665X/aadf05.

[14] Y. Han, W. Lu, Optimizing the deformation behavior of stent with nonuniform Poisson's ratio distribution for curved artery, J. Mech. Behav. Biomed. Mater. (2018).

[15] Y. Han, W. Lu, Evolutionary design of nonuniform cellular structures with optimized Poisson's ratio distribution, Mater. Des. 141 (2017) 384–394. doi:10.1016/j.matdes.2017.12.047.

[16] S. Akbari, A.H. Sakhaei, K. Kowsari, B. Yang, A. Serjouei, Z. Yuanfang, Q. Ge, Enhanced multimaterial 4D printing with active hinges, Smart Mater. Struct. 27 (2018). doi:10.1088/1361-665X/aabe63.

[17] Y. Han, W. Lu, Evolutionary design of nonuniform cellular structures with optimized Poisson's ratio

distribution, Mater. Des. 141 (2018) 384–394. doi:10.1016/j.matdes.2017.12.047.
[18] L. Piegl, W. Tiller, The NURBS Book , (1997). doi:10.1007/978-3-642-59223-2.